Long-term evaluation of the Hydro-Thermodynamic Soil-Vegetation Scheme's frozen ground/permafrost component using observations at Barrow, Alaska

Nicole Mölders and Vladimir E. Romanovsky

Geophysical Institute, University of Alaska Fairbanks, Fairbanks, Alaska, USA

Received 8 March 2005; revised 23 September 2005; accepted 28 October 2005; published 28 February 2006.

[1] The multi-layer frozen ground/permafrost component of the hydro-thermodynamic soil-vegetation scheme (HTSVS) was evaluated by means of permafrost observations at Barrow, Alaska. HTSVS was driven by pressure, wind, air temperature, specific humidity, snow-depth, rain, downward shortwave and long-wave radiation observations for 14 consecutive years. Observed soil temperature data are available at various times during this period. HTSVS predicts soil temperatures that are slightly too low with root mean square errors (RMSEs) of, on average, less than 3.2 K. Sensitivity studies suggest that the treatment of snow and vegetation cover may be reasons for the inaccuracy. HTSVS' original thermal conductivity parameterization provides thermal conductivity values that are too high compared to typical observations. Introducing a parameterization frequently used in the permafrost research community, which was modified for application in numerical weather prediction (NWP) and climate models and model consistency in HTSVS, improves soil temperature predictions and reduces RMSEs in some layers by up to 1 K, and on average by 0.2 K. Assuming five to ten layers for the first 2 or 3 m as is usually done in NWP and climate modeling is insufficient to capture the active layer depth, because the number and position of the grid nodes play a role. The depth of the lower boundary of the soil model and the boundary condition affect the overall performance. Consequently, under current computational possibilities, simulating permafrost and the active layer in atmospheric models requires a compromise between the degree of accuracy and affordable computational time.

Citation: Mölders, N., and V. E. Romanovsky (2006), Long-term evaluation of the Hydro-Thermodynamic Soil-Vegetation Scheme's frozen ground/permafrost component using observations at Barrow, Alaska, *J. Geophys. Res.*, *111*, D04105, doi:10.1029/2005JD005957.

1. Introduction

[2] At high latitudes, permafrost, soil in which temperatures remain below 0°C for at least two consecutive years, and the active layer, which thaws seasonally, are the primary subsurface components of the land-atmosphere system. The associated thermal and hydrological conditions affect climate by the exchange of heat, moisture, and matter [e.g., *Stendel and Christensen*, 2002; *Mölders and Walsh*, 2004]. At the same time, permafrost temperature and stability and active layer depth are sensitive to climatic change [e.g., *Kane et al.*, 1991]. Atmospheric warming may start permafrost warming, and change the long-term mean surface temperature with feedbacks to climate and other potential impacts. Permafrost thawing, for instance, can cause huge economic and infrastructure damages and ecosystem changes, and affects trace gas and water cycles [*Esch and Osterkamp*, 1990; *Cherkauer and Lettenmaier*, 1999; *Oechel et al.*, 2000; *Serreze et al.*, 2000; *Romanovsky and Osterkamp*, 2001; *Zhuang et al.*, 2001]. To appropriately describe heat, moisture, and matter exchange at the surface-atmosphere interface in the Arctic and to examine permafrost-climate feedbacks, modern climate models require suitable land-surface models (LSMs) to simulate frozen ground and permafrost dynamics.

[3] In recent decades geologists and geophysicists have exerted great effort to develop site-specific permafrost models to examine permafrost dynamics [e.g., *Goodrich*, 1982; *Nelson and Outcalt*, 1987; *Kane et al.*, 1991; *Romanovsky and Osterkamp*, 1997; *Smith and Riseborough*, 2001; *Zhuang et al.*, 2001; *Ling and Zhang*, 2003]. Detailed permafrost models (1) usually require a large amount of computational time because of their fine vertical resolution ($\leq$0.05 m), (2) typically run at large time steps due to geologically slow processes, (3) are site-specific, and (4) have to be calibrated [e.g., *Romanovsky et al.*, 1997; *Osterkamp and Romanovsky*, 1999; *Romanovsky and Osterkamp*, 2001]. In calibration, a great part of a data set is used to determine optimal soil-transfer parameters, leaving a lesser part for model evaluation.

[4] Applying a typical calibration technique certainly would lead to better predictions than those presented here.

0148-0227/06/2005JD005957$09.00

However, climate prediction with calibrated LSMs or coupling calibrated permafrost models to climate models would require consistent soil temperature data for calibration on a global scale. Since as of today no such data set exists, usage of calibrated permafrost models in climate models is technically impossible. Therefore, and since calibration coefficients may be climate sensitive, the climate-modeling community does not use calibration techniques in models that are applied in climate-system modeling. In addition, permafrost and climate models are not coupled because climate simulations require input of water and energy fluxes to the atmosphere at time steps of several minutes or so. Thus, a vertically highly-resolved permafrost model would have to run with this much smaller time-step making synchronous simulations by a climate model coupled with a permafrost model computationally prohibitive.

[5] Apparently high-latitude terrestrial processes, especially those related to permafrost variations, have yet to receive a concerted effort within the context of global climate modeling. Studies carried out with the standalone versions of 21 state-of-the-art LSMs using soil temperature observations along with fluxes and snow data from the 18-year Valdai data set, collected at a site without permafrost but with regularly frozen ground in winter, showed that explicit inclusion of soil-water freezing improves simulations of soil temperature and its variability at seasonal and inter-annual scales [*Luo et al.*, 2003]. For all these reasons permafrost, permafrost dynamics, and soil-water freezing/thawing must be considered in climate assessment.

[6] To achieve this goal, knowledge and well-accepted concepts from permafrost and atmospheric sciences can be combined to build a suitable soil model for use in climate and Arctic numerical weather prediction (NWP) models. Recently, *Mölders et al.* [2003a] developed a frozen ground/permafrost component for the HTSVS [*Kramm et al.*, 1994, 1996] for simulating soil processes including freezing and thawing and soil-heat conduction in NWP and climate models. In the present study, we evaluate HTSVS' performance in simulating the dynamics associated with permafrost and the active layer by using long-term soil-temperature observations made at Barrow, Alaska (USA), a site with cold permafrost conditions.

2. Method

2.1. Brief Model Description

[7] HTSVS [e.g., *Kramm et al.*, 1994, 1996; *Mölders et al.*, 2003a; *Mölders and Walsh*, 2004] describes the exchange of momentum, heat, and moisture at the vegetation-soil-atmosphere interface, with special consideration given to the heterogeneity on the micro-scale by the Deardorff-type mixture approach, i.e., a grid cell can be partly covered by vegetation [*Deardorff*, 1978; *Kramm et al.*, 1996]. It considers snow's insulating effect and retardation of infiltration by a multi-layer snow model, water uptake by plants including a vertically variable vegetation-type dependent root distribution, and the temporal variation of soil albedo and snow albedo and emissivity. In addition to mineral soils, HTSVS can consider organic soil layers (e.g., moss, lichen, peat) [*Mölders and Walsh*, 2004] that are of special relevance for the moisture distribution within soils and permafrost dynamics [e.g., *Beringer et al.*, 2001].

[8] The multi-layer soil model considers the (vertical) heat- and water-transfer processes (including the Richards equation) [*Kramm et al.*, 1994, 1996], and soil freezing/thawing [*Mölders et al.*, 2003a] based on the principles of the linear thermodynamics of irreversible processes [e.g., *de Groot*, 1951; *Prigogine*, 1961]. The governing balance equations for heat and moisture including phase transition processes and water extraction by roots χ are [e.g., *Philip and de Vries*, 1957; *de Vries*, 1958; *Sasamori*, 1970; *Flerchinger and Saxton*, 1989; *Kramm et al.*, 1994, 1996; *Mölders et al.*, 2003a],

$$C\frac{\partial T_S}{\partial t} = \frac{\partial}{\partial z_S}\left(\lambda\frac{\partial T_S}{\partial z_S}\right) + \frac{\partial}{\partial z_S}\left(L_v\rho_w D_{T,v}\frac{\partial T_S}{\partial z_S}\right) + \frac{\partial}{\partial z_S}\left(L_v\rho_w D_{\eta,v}\frac{\partial \eta}{\partial z_S}\right) + L_f\rho_{ice}\frac{\partial \eta_{ice}}{\partial t} \quad (1)$$

$$\frac{\partial \eta}{\partial t} = \frac{\partial}{\partial z_S}\left(D_{\eta,v}\frac{\partial \eta}{\partial z_S}\right) + \frac{\partial}{\partial z_S}\left(D_{\eta,w}\frac{\partial \eta}{\partial z_S}\right) + \frac{\partial}{\partial z_S}\left(D_{T,v}\frac{\partial T_S}{\partial z_S}\right) + \frac{\partial K_w}{\partial z_S} - \frac{\chi}{\rho_w} - \frac{\rho_{ice}}{\rho_w}\frac{\partial \eta_{ice}}{\partial t} \quad (2)$$

Here z_S, λ, L_v, L_f, T_S, η, η_{ice}, $D_{\eta,v}$, $D_{\eta,w}$ and $D_{T,v}$ are soil depth, thermal conductivity, latent heat of condensation and freezing, soil temperature, volumetric water and ice content, and the transfer coefficients for water vapor, water, and heat. Soil hydraulic conductivity $K_w = k_s W^{2b+3}$ depends on the saturated hydraulic conductivity, k_s, the relative volumetric water content $W = \eta/\eta_s$, porosity η_s and pore-size distribution index b [e.g., *Clapp and Hornberger*, 1978; *Dingman*, 1994]. The volumetric heat capacity of moist soil [*Mölders et al.*, 2003a]

$$C = (1-\eta_s)\rho_S c_S + \eta\rho_w c_w + \eta_{ice}\rho_{ice}c_{ice} + (\eta_s - \eta - \eta_{ice})\rho_a c_p \quad (3)$$

is a function of the density ρ_S, ρ_w, ρ_{ice}, and ρ_a and specific heat capacity c_S, c_w, c_{ice}, and c_p of the dry soil material, water, ice and air. The thermal conductivity of unfrozen ground depends on water potential $\psi = \psi_s W^{-b}$ [*McCumber*, 1980]

$$\lambda = \begin{cases} 419\exp(-(P_f+2.7)) & P_f < 5.1 \\ 0.172 & P_f \geq 5.1 \end{cases} \quad (4)$$

with ψ_s being the saturated water potential and $P_f = 2 + {}^{10}\log|\psi|$. At soil temperatures below 0°C, a mass-weighted thermal conductivity depending on volumetric ice and water content is calculated using equation (4) for the liquid and 2.31 J/(msK) for the solid phase. The transfer coefficients are given by [*Philip and de Vries*, 1957; *Kramm*, 1995]

$$D_{\eta,v} = -\alpha\nu D_w b\frac{\eta_s - \eta}{\eta}\frac{\rho_d}{\rho_w}\frac{g\psi}{R_d T_S} \quad (5)$$

$$D_{\eta,w} = -\frac{bk_s\psi_s}{\eta}\left(\frac{\eta}{\eta_s}\right)^{b+3} \quad (6)$$

$$D_{T,v} = \alpha\nu D_w(\eta_s - \eta)\frac{\rho_d}{\rho_w}\frac{L_v - g\psi}{R_d T_S{}^2} \quad (7)$$

where g is the acceleration due to gravity, α, ν, D_w, ρ_d, and R_d are the torsion factor that considers curvatures in the soil material due to roots [*Sasamori*, 1970; *Zdunkowski et al.*, 1975; *Sievers et al.*, 1983; *Kramm et al.*, 1996], a correction factor that is typically close to 1 and hence assumed to be 1, the molecular diffusion coefficient of water vapor in moist air, and the density and gas constant for dry air.

[9] At a given soil temperature below 0°C all water in excess of [*Flerchinger and Saxton*, 1989]

$$\eta_{max} = \eta_s \left\{ \frac{L_f (T_S - 273.15)}{g \psi_s T_S} \right\}^{-1/b} \tag{8}$$

is frozen (Figure 1).

[10] In equation (1), the first term on the right side describes soil temperature changes by divergence of soil-heat fluxes. The second term represents the divergence of soil-heat fluxes due to water-vapor transfer. The third term describes how a soil moisture gradient contributes to the soil-temperature change (Dufour effect), and the last term addresses soil temperature changes due to freezing/thawing. In equation (2), the first two terms on the right side represent the changes in volumetric water content caused by divergence of water vapor and water fluxes. The third term describes how a temperature gradient contributes to the change in volumetric water content (Ludwig-Soret effect). The saturation vapor pressure depends on soil temperature. Thus, a gradient in soil temperature leads to differences in saturation pressure and a water vapor flux that affects soil moisture. This phenomenon, well known to occur in snow, also exists in soils [*Philip and de Vries*, 1957; *de Vries*, 1958]. The fourth term represents changes due to hydraulic conductivity, the fifth gives water uptake by roots, and the last considers changes due to freezing/thawing. The Ludwig-Soret and Dufour effects are cross-phenomena usually considered in the thermodynamics of irreversible processes.

[11] The number of model layers can be arbitrarily chosen. In the reference simulation (CTR), the uppermost soil-layer ranges from the Earth's surface to the uppermost level within the soil at 0.01 m depth. Between that level and lowest level at 20m depth, all 20 layers are spaced by the same logarithmic increment so that central differences can be used in solving the coupled equations (1) and (2) by a generalized Crank-Nicholson scheme. In this configuration soil-layer boundaries are at approximately 0, 0.01, 0.015, 0.02, 0.03, 0.05, 0.07, 0.11, 0.16, 0.25, 0.37, 0.55, 0.82, 1.22, 1.81, 2.71, 4.04, 6.02, 8.99, 13.41, and 20 m depth. If not mentioned differently, soil temperature and relative volumetric water and ice content are held constant at −9.5°C, 0.06, and 0.817 $m^3\ m^{-3}$ at the lower boundary of the soil model at 20 m depth throughout the entire simulation time in accordance with observations [*Romanovsky et al.*, 2002]. This grid and these boundary conditions are used in the reference simulation.

[12] HTSVS calculates snow albedo α_{snow} in accord with *Luijting et al.* [2004] and *Mölders et al.* [2003a] for reference height air temperature T_R below and above the freezing point

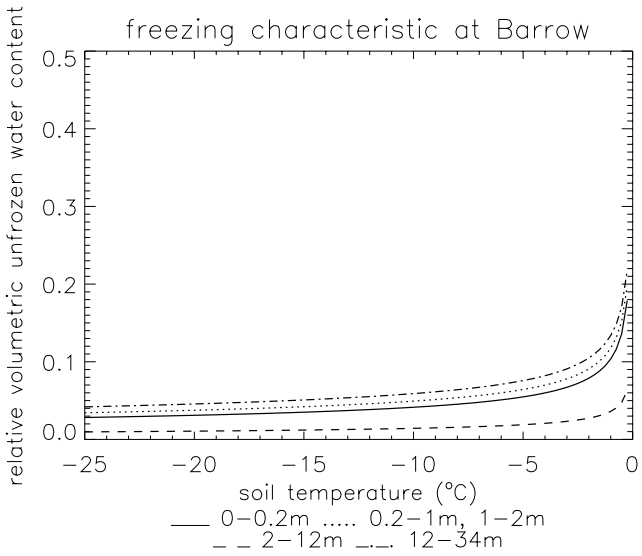

Figure 1. Dependence of freeze-thaw characteristic curve at various depths as obtained by equation (8) normalized with the porosity derived from the Barrow soil analysis on soil temperature and relative volumetric water content ($W = \eta/\eta_s$). Relative volumetric water content is dimensionless.

$$\alpha_{snow}(t) = \begin{cases} 0.63 + 0.0011 T_R + 0.01 h_s - 0.009 v + 4.492 \cdot 10^{-7} t_{snow} & \text{for } T_R < 273.15\text{K} \\ 0.35 + 0.18 \exp\left(\dfrac{-t_{snow}}{114048}\right) + 0.31 \exp\left(\dfrac{-t_{snow}}{954720}\right) & \text{for } T_R \geq 273.15\text{K}. \end{cases} \tag{9}$$

Here v is wind speed, and t_{snow} is the time after the last snow event. *Luijting et al.*'s formula was derived from daily averages of downward and upward shortwave radiation measured between 2001 and 2002 at the Atmospheric Radiation Measurement (ARM) program [*Ellingson et al.*, 1999] site. *Mölders et al.*'s formula was derived from data measured by the *U.S. Army Corps of Engineers* [1956] in the contiguous United States in the 1950's (see *Mölders et al.* [2003a] for details).

2.2. Site Description

[13] The permafrost site at Barrow (71°18′N, 156°47′W, 5m a.s.l.) is located in fairly flat and sodden terrain, with continuous cold permafrost and numerous thaw lakes. The uppermost 0.2 m thick soil layer consists of silt with traces of organic material. Underneath this mixed layer a layer of pure silt is located that reaches to 2 m depth. Below 2 m depth, a 10 m thick layer follows made up of a mixture of sand, gravel and some silt. Silt with some sand occurs from 12 to 34 m depth. The soil physical parameters (Table 1) used in this study are derived from the quantities determined by inverse solution modeling [*Osterkamp and Romanovsky*, 1997]. The freeze-thaw characteristic curves at various depths as obtained by using the parameters of Table 1 in equation (8) normalized with porosity (Figure 1) hardly differ from the freeze-thaw curves derived for this site by *Romanovsky and Osterkamp* [2000] using variations in soil temperature within the active layer and near-surface permafrost.

[14] Barrow has an Arctic climate. For the last climate period (1971–2000), the annual mean wind speed was

Table 1. Soil Parameters as Used in the Simulations for Barrow[a]

Depth, m	Material	η_s, $m^3\ m^{-3}$	$c_s\ \rho_s$, $10^6 J/(m^3 K)$	b, -.-	k_s, $10^{-6} m/s$	ψ_s, m	λ_s, W/(mK)
0–0.2	silt with organics	0.6	0.85086	2.545	1.134	−0.389	1.0497
0.2–1	silt	0.55	0.971071	2.6875	2.493	−0.396	0.7536
1–2	silt	0.55	0.971071	2.6875	1.869	−0.396	0.9791
2–12	sand, gravel, some silt	0.55	0.971071	2.6	141.000	−0.030	0.9376
12–34	silt and some sand	0.44	1.159974	2.85	91.620	−0.405	0.6137

[a]The letters η_s, $c_s\rho_s$, b, k_s, ψ_s, and λ_s stand for porosity, dry soil volumetric heat capacity, pore-size distribution index, saturated hydraulic conductivity, saturated water potential, and thermal conductivity of the dry soil material, respectively.

7.6 m/s; it is generally windy, with fall being the windiest season. On average, annual mean air temperature is −12°C. Generally, February is the coldest (−26.6°C) and July the warmest month (4.7°C). Air temperatures remain below 0°C through most of the year, with daily maxima exceeding 0°C on 109 days per year. Annual average precipitation amounts to 105 mm, of which on average 74 mm falls as snow year round. Transition from snow to snow-free conditions occurs in late May/early June. Barrow receives no sunlight between 18 November and 24 January, and constant sunlight between 10 May and 2 August.

2.3. Soil Temperature Data

[15] Daily averages of soil temperature are available for 18 August 1993 to 9 August 1996, and 21 August 1998 to 17 August 1999 at 0.01, 0.08, 0.15, 0.22, 0.29, 0.55, 0.75, and 1 m depth [*Hinkel et al.*, 2001]. Hourly measurements are available at the surface, 0.04, 0.1, 0.17, 0.24, 0.32, 0.4, 0.47, 0.55, 0.7, 0.85, and 1.08 m for 11 August 2002 0900 UT to 11 August 2003 0800 UT from the Barrow Permafrost Observatory of the International Arctic Research Center [e.g., *Yoshikawa et al.*, 2004]. Soil temperature measurements have an accuracy of ±0.5K. Since sensible and latent heat flux or runoff are of marginal interest for permafrost scientists, these quantities were not measured at the Barrow Permafrost Observatory.

2.4. Forcing Data

[16] Forcing data are available from 1 January 1990 to 31 December 2003. Observed wind, air and dew point temperatures, and pressure data are taken from the Barrow Climate Monitoring and Diagnostics Laboratory (CMDL) site. The CMDL site is 11 m above sea level, and was 100 m and 1 km away from the permafrost site for data recorded in the 90's and from 2000 onwards, respectively. Note that the permafrost site was moved in 2000. Air and dew point temperatures were measured in aspirated sun shields at 2 m height. Missing data were linearly interpolated. Specific humidity was derived from dew-point temperature using the psychrometer formula.

[17] Precipitation amount was measured with an unheated tipping bucket rain gauge; i.e., no solid precipitation was reported at the permafrost site. Due to the large snowfall catch deficiencies [e.g., *Yang and Woo*, 1999; *Yang et al.*, 2000; *Sugiura and Yang*, 2003], and because no snowfall data were available at the permafrost sites, we drove HTSVS with snow depth measured at the Barrow CMDL site and used only observed liquid precipitation. To ensure that snow depth only changes when a change in snow depth was reported, we determined snow density according to equation (9) in *Mölders and Walsh* [2004]. We did not explicitly calculate compaction, settling and melt-water percolation as usually performed by HTSVS, because these processes would alter snow depth in HTSVS' original formulation. When no change in snow depth was reported, but outflow and/or sublimation were predicted by HTSVS, snow density was reduced in the simulation for continuity reasons to ensure conservation of water ($h_s\ \rho_s = \rho_w\ h_w$ where h_s and h_w are snow depth and height of snow water equivalent). Because of this necessity, snow density could not be used for calculation of snow thermal conductivity; instead we used a constant value of 0.14 W/(Km) [*Lee*, 1978]. When a new snowpack was reported, initial snow density was treated in accord with *Mölders and Walsh* [2004].

[18] Radiation data are taken from the Barrow ARM site, which is at the same location as the CMDL site. Down-welling shortwave radiation was measured at 1-min intervals by an unshaded pyranometer with a hemispheric field of view and an inverted Eppley Laboratory, Inc., Precision Spectral Pyranometer (PSP). This instrument measures in a nominal wavelength range of 0.3–2.8 micrometers with a response time, sensitivity, and uncertainty of 1-s, ~9 $\mu V/Wm^{-2}$, and ±3% or 10 Wm^{-2}, respectively. Short-wave radiation may be underestimated during snow events and snow blow as these events cover the radiometer with snow.

[19] Down-welling long-wave radiation is measured between 40 and 50 micrometers by a shaded pyrgeometer with hemispheric field of view. Downward long-wave radiation data are available as 3-min averages until 12/31/1997 and as 1-min averages since 1/1/1998. Occasionally missing data were substituted by downward long-wave radiation calculated in accord with *Eppel et al.* [1995]. Since no data on cloud fraction were available, we assumed an average cloudiness of 80% in parameterization of downward long-wave radiation. Thus, calculated downward long-wave radiation will be under/overestimated for more/less than 80% cloud fraction.

2.5. Meteorological Conditions

[20] During our episode, annual average downward short-wave and long-wave radiation, air temperature, and wind speed were 96.9 Wm^{-2}, 224 Wm^{-2}, −11.5°C, and 5.7m/s, respectively. This period was slightly warmer (0.5 K) and calmer (1.9 m/s) than the 1971–2000 average.

[21] The episode 2002/03 was the warmest and 1994/95 the coldest (Table 2); the average air temperatures of 1993/94, 1995/96, and 1998/99 hardly differ. The mean specific humidity differs only slightly for the first four observational episodes (0.004 g/kg at maximum), while that for 2002/03 is 0.01 g/kg higher than that for the driest episode (1994/95). This results from the fact that warmer air can take

Table 2. Averages of Atmospheric Conditions for the Five Observational Episodes[a]

Episode	Air Temperature, °C	Specific Humidity, g/kg	Wind Speed, m/s	Snow Depth, mm	Downward Shortwave Radiation, W m^{-2}	Downward Long-Wave Radiation, W m^{-2}	Number of Snow-Cover Days, -.-
1993/94	−11.1	0.225	6.20	142	96.4	271.1	167
1994/95	−12.9	0.224	5.31	129	93.1	247.3	186
1995/96	−11.1	0.226	5.33	138	92.3	237.4	204
1998/99	−11.0	0.228	5.11	123	98.6	238.7	221
2002/03	−9.8	0.234	5.88	143	96.7	252.7	183

[a]Note that averages are calculated for the observational episodes and not for hydrological years.

up more water vapor than relatively colder air before saturation occurs. Averaged snow depth was about 8% higher in 1993/94 and 2002/03, and about 8% lower in 1998/99 than in 1994/95 or 1995/96. The number of days with reported snow depth strongly differs for our observational episodes (Table 2). Averaged mean wind speed was about the same for the episodes 1994/95, 1995/96, and 1998/99, while it was appreciably higher in 1993/94 and 2002/03. Average insolation differs by up to 6 Wm^{-2} between the observational episodes. Annual accumulated rain was more than 8% higher in 1993/94 and 1998/1999 than for the other observational episodes.

2.6. Initialization

[22] The model was started using a climatologic soil temperature profile and assuming that all pores are filled with water and/or ice. HTSVS was forced by 1990 data, repeating that year three times to reach equilibrium between soil temperatures, volumetric water and ice content and climate (model spin-up). Soil temperatures predicted for the third repeated year hardly (<0.001 K) differ from the second year's temperatures. The second and first year's soil temperatures differ by 0.5 K (0.1, 0.05, 0.01, 0.005 K) after 1 day (77, 137, 199, 210 days) of the second year. Since the differences between the first and the second year are already less than 0.5 K after 1 day, we conclude that the model responds well to the atmospheric forcing, and that it quickly achieves an acceptable equilibrium between soil and atmosphere. The 0.5 K discrepancy is of the same magnitude as the error typical for routine soil temperature measurements. We use the soil temperature, volumetric water and ice content, snow temperature and density obtained at the end of this three year spin-up as initial conditions for the simulations that continuously run from 1 January 1990 to 31 December 2003. Note that soil temperature results obtained without the spin-up hardly differ from those presented here.

2.7. Evaluation

[23] HTSVS was driven by hourly averages of wind, air temperature, specific humidity, pressure, rain, snow depth, and downward shortwave and long-wave radiation. Daily averages of simulated and observed soil temperatures were compared for various depths. We performed sensitivity studies on vertical grid resolution, assumptions and simplifications typically made in NWP and climate modeling, and parameterizations to (1) assess their impact on the model outcome, and (2) identify model deficits and limitations of predictability.

[24] Systematic and non-systematic errors contribute to the prediction error. To quantify the model errors we calculate the bias

$$\bar{\phi} = \frac{1}{n}\sum_{i=1}^{n}\phi_i \tag{10}$$

root-mean-square error

$$\mathrm{RMSE} = \left(\frac{1}{n-1}\sum_{i=1}^{n}(\phi_i)^2\right)^{1/2} \tag{11}$$

and the standard deviation of error

$$\mathrm{SDE} = \left(\frac{1}{n-1}\sum_{i=1}^{n}\left(\phi_i - \bar{\phi}\right)^2\right)^{1/2} \tag{12}$$

Here ϕ_i is the difference between the ith predicted and observed soil temperature and n is the total number of observations. The bias represents systematic errors from consistent misrepresentation of geometrical, physical, or numerical factors, while SDE represents random errors caused by uncertainty in initial and boundary conditions or observations. RMSE evaluates overall performance and prevents positive and negative errors from cancelling each other out.

3. Results

3.1. General Remarks

[25] Temperature and moisture states evolve by fluxes which themselves depend on those states [*Entekhabi and Brubaker*, 1995]. Thus, false predictions of soil temperature and moisture profiles can produce incorrect phase transition processes and soil-heat and moisture fluxes that propagate in incorrect water and energy fluxes to the atmosphere, and hence limit the reliability of NWP or climate models. Therefore a soil model has to be evaluated at various temporal scales for a wide range of climate conditions. Evaluation of HTSVS by data on mean values of wind speed, temperature, and humidity, and on eddy flux densities (the so-called eddy fluxes) of momentum, sensible heat, and water vapor gathered during the Great Plains Turbulence Project, GREIV I-1974 (GREnzschicht Instrumentelle Vermessung phase I, i.e., first phase of probing the atmospheric boundary layer) [e.g., *Kramm*, 1995], SANA (SANierung der Atmosphäre über den neuen Bundesländer, i.e., recovery of the atmosphere over the new federal countries) [e.g., *Spindler et al.*, 1996], CASES97 (Cooperative Atmosphere Surface Exchange Study 1997) [e.g.,

Table 3. Statistics on Model Performance[a]

	RMSE, K	Bias, K	SDE, K	F-Statistic	Significance	r	Offset of Thaw-Up, d	Offset of Freeze-Up, d
CTR	3.2	−1.3	2.9	1.099	0.168	0.933	−13.2	−5.0
CTR-EQ4	3.4	−0.1	3.4	1.067	**0.020**	0.908	−13.2	−5.2
S10-3	4.0	−2.6	3.1	1.100	**0.003**	0.931	−13.0	−4.2
S10-2	3.4	−1.7	3.0	1.075	**0.008**	0.930	−13.2	−5.0
S10-20	3.1	−1.2	2.8	1.074	0.189	0.936	−13.0	−4.4
SHOM	3.4	−1.3	3.1	1.170	**0.035**	0.925	−13.2	−5.4
SB3L10	2.8	0.1	2.8	1.103	0.166	0.937	−13.2	−4.8
SB2L10	3.1	−0.5	3.0	1.065	**0.060**	0.930	−13.4	−4.2
SB3L5	3.2	−0.3	3.2	1.175	**<0.001**	0.931	−13.4	−4.4
SNWTHC	4.0	−2.3	3.3	1.151	**<0.001**	0.926	−13.2	−5.6
SNWHS	3.1	−1.0	3.0	1.128	**0.003**	0.930	−13.0	−5.2
S5SNL	3.3	−1.3	3.0	1.047	0.209	0.929	−13.0	−5.6
SALB	3.2	−1.9	2.6	1.025	0.274	0.946	−13.0	−5.2

[a]RMSE, bias, standard deviation error SDE, F-statistic, significance, and Pearson correlation coefficient r are calculated over all depths and the entire time for which soil temperature observations are available. The F-statistic and significance calculation refer to the success of HTSVS to predict the same time series of temperature variations. Simulations with statistically significant (at the 90% or higher confidence level) different temporal evolution are given in bold. The mean offset (simulated-observed) for onset of thawing and freezing is given for the uppermost soil layer and averaged over all seasons for which observational data are available. CTR, S10-3, S10-2, S10-20 refer to the reference simulation, the simulations with a lower boundary at 20 m depth and 10 layers in the uppermost 3, 2 and 20 m, respectively; S5-3 has five layers to 3 m depth. SHOM assumes the same soil properties throughout the column. CTR-EQ4 uses equation (4) for thermal conductivity. SB3L10 and SB2L10 have 10 layers and the bottom of the soil model at 3 and 2 m depth. SB3L5 has five layers and the bottom of the soil model at 3 m depth. SALB uses *Mölders et al.*'s [2003a] snow albedo parameterization. S5SNL considers five instead of three snow model layers. SNWTHC uses 0.42 W/(mK) as snow thermal conductivity, SNWHS assumes a 10% increase in snow depth.

LeMone et al., 2000] and BALTEX (BALTic sea EXperiment) [e.g., *Raschke et al.*, 1998] showed that HTSVS accurately simulates the diurnal course of state variables and fluxes [*Kramm*, 1995; *Mölders*, 2000; *Narapusetty and Mölders*, 2005]. By using lysimeter data from a midlatitude site with occasionally frozen ground in winter *Mölders et al.* [2003a, 2003b] found that HTSVS predicts the long-term (2050 days) accumulated sums of evapotranspiration and recharge with better than 15% accuracy. Soil temperatures were predicted within 1–2 K accuracy, on average [*Mölders et al.*, 2003b].

[26] The suitability for long-term integration can only be evaluated using routine data because sophisticated field experiments cannot be performed continuously over years. Due to logistic difficulties routine data are often less accurate than data collected in special field experiments where scientists stand by to immediately fix problems (e.g., remove snow from the radiometer, replace failing parts, check data logger). Field experiments are usually designed for a particular evaluation or to answer a question; all required model data are measured and quantities are rather over- than underdetermined. When using routine data often some data needed as model input or forcing are unavailable or not available with sufficient resolution. Consequently, evaluations based on routine data will never yield results as good as those based on data from a good field experiment [e.g., *Spindler et al.*, 1996; *Slater et al.*, 1998; *Mölders et al.*, 2003b].

3.2. Systematic Errors and Overall Performance

[27] Since rain data are only available as daily accumulated values, hydrological and energetic consequences of the unknown temporal evolution of rain may cause discrepancies between simulated and observed soil temperature. The consequences for soil moisture and runoff have been discussed elsewhere [e.g., *Mölders and Raabe*, 1997; *Mölders et al.*, 1999]. Inaccurately measured rain due to catch deficiencies or traces of rain and great snowfall spatial variability known for Arctic regions and Barrow may cause similar errors.

[28] Except for some sensitivity studies HTSVS has a cold bias (Table 3). There are several reasons: (1) In nature, snow thermal conductivity depends on snow density and temperature [*Sturm et al.*, 1997], while we used a constant value (0.14 W/(mK)) for the reasons outlined in section 2.4. Therefore snow-heat fluxes (counted positive when downward) toward the soil will be overestimated if natural thermal conductivity is higher than the model value, and vice versa. This uncertainty is unavoidable as no measurements of snow thermal conductivity were available. (2) During snow events and snow blow, measured long-wave radiation values may be too small if the radiometer is snow-covered. These measurement errors in the forcing data cause systematic errors in predicted soil temperature toward colder values (see SDE in Table 3). (3) Water vapor may deposit onto radiometers as frost leading to underestimation of downward long-wave radiation that finally contributes to the cold bias. Note that $50 Wm^{-2}$ average lower downward long-wave radiation can lead to a doubling of the frequency of days with soil temperatures below 0°C, an underestimation of soil temperature, and an overestimation of frost depth [*Mölders et al.*, 2003b] in midlatitude winter.

[29] On average, HTSVS simulates onset of thaw-up and freeze-up about 13 and 5 days too early (Table 3). Sensitivity to simulation setup is marginal; ±1 day for thaw-up, ±3 days for freeze-up. Average onset of thaw-up is 31, 8, 8, 15, and 3 days, and of freeze-up 4, 3, 10, 5, and 3 days too early for 1994, 1995, 1996, 1999, and 2003, respectively (e.g., Figure 2). There are several reasons for premature thaw-up: (1) Incorrect snow depth forcing may greatly contribute to premature thawing. As pointed out, snow depth was measured 100 m (1990's) and 1000 m (2000 onwards) away from the permafrost site. The snow depth site is 6 m higher than the permafrost site, so snow easily gets blown away, while it deposits at the permafrost site. Snow-depth reports usually stop when snow cover becomes

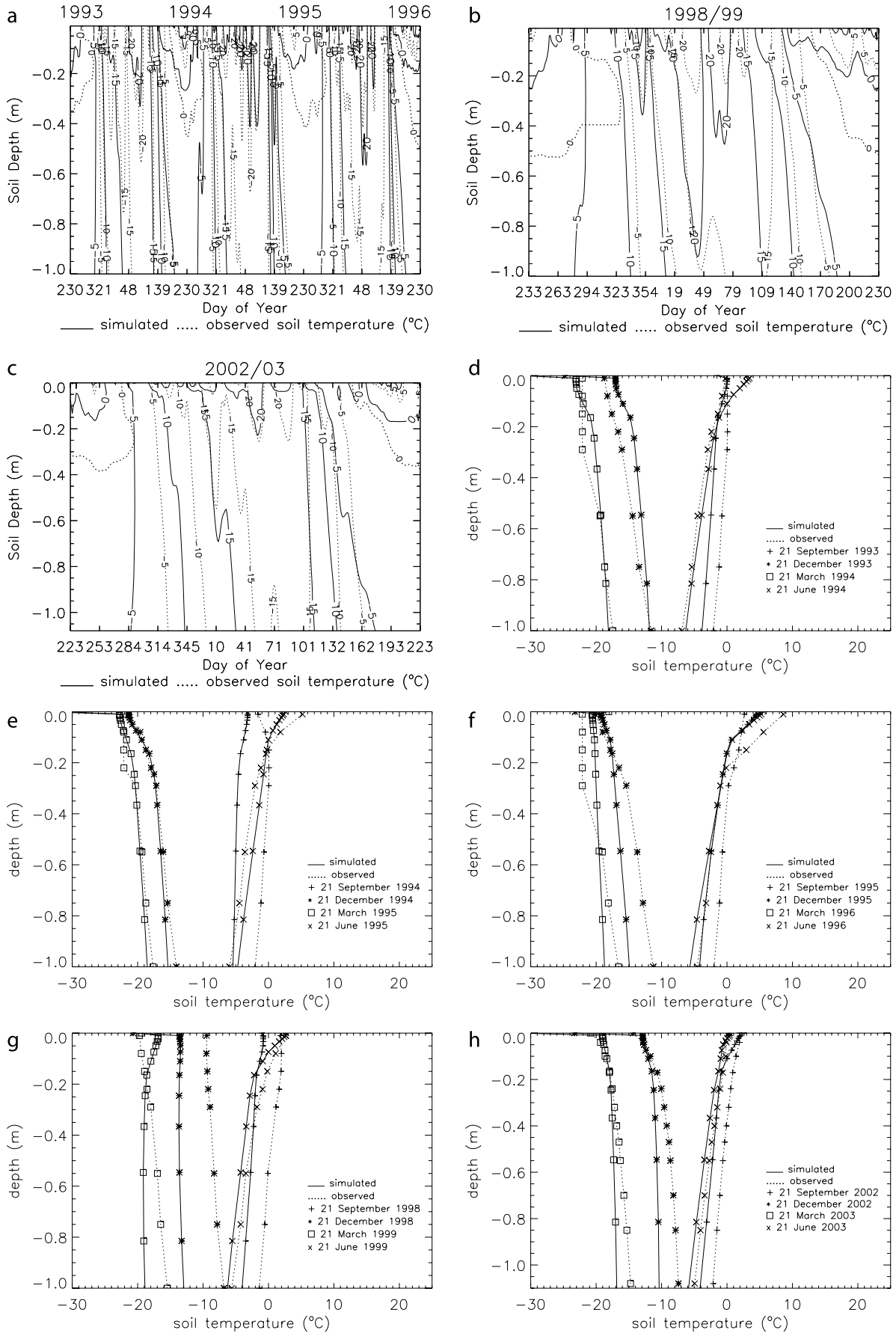
a
1993
1994
1995
1996
Soil Depth (m)
Day of Year
simulated ..... observed soil temperature (°C)
b
1998/99
Soil Depth (m)
Day of Year
simulated ..... observed soil temperature (°C)
c
2002/03
Soil Depth (m)
Day of Year
simulated ..... observed soil temperature (°C)
d
depth (m)
soil temperature (°C)
simulated
observed
+ 21 September 1993
* 21 December 1993
□ 21 March 1994
x 21 June 1994
e
depth (m)
soil temperature (°C)
simulated
observed
+ 21 September 1994
* 21 December 1994
□ 21 March 1995
x 21 June 1995
f
depth (m)
soil temperature (°C)
simulated
observed
+ 21 September 1995
* 21 December 1995
□ 21 March 1996
x 21 June 1996
g
depth (m)
soil temperature (°C)
simulated
observed
+ 21 September 1998
* 21 December 1998
□ 21 March 1999
x 21 June 1999
h
depth (m)
soil temperature (°C)
simulated
observed
+ 21 September 2002
* 21 December 2002
□ 21 March 2003
x 21 June 2003

Figure 2

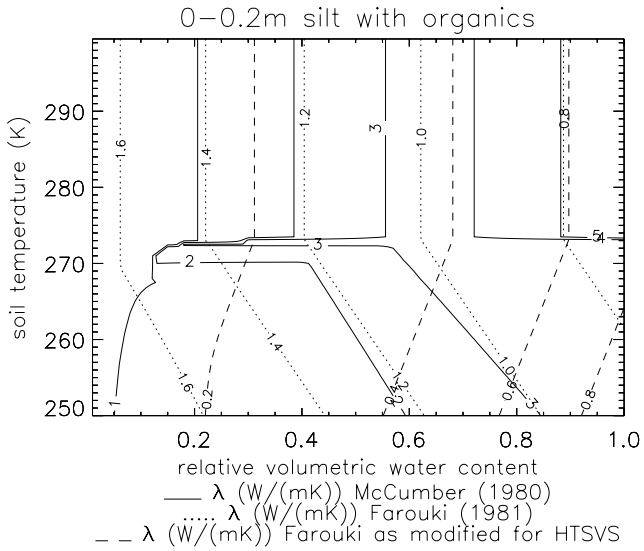

Figure 3. Thermal conductivity as obtained by equations (4) and (13). Figures for other soil layers show the same basic pattern.

patchy; therefore there may be still snow at the permafrost site although snow-depth reports indicate none. Advancing snow cover disappearance by 10 days can increase maximum soil temperature up to 6.6, 2.2, 1.5, and 0.7 K and annual means by 0.2, 0.2, 0.1, and 0.1 K at the surface, 0.5, 1, and 2 m depth [*Ling and Zhang*, 2003]. These values are within the range of our discrepancies. (2) The urban effect may accelerate snowmelt [*Hinkel et al.*, 2003] at the snow-depth site as compared to the permafrost site farther away from town. (3) At Barrow, trace precipitation varies spatially and occurs with high frequency [e.g., *Yang and Woo*, 1999; *Sugiura and Yang*, 2003]. Thus, the systematic errors of gauge-measured rain include not only wind-induced undercatch, wetting, and evaporation losses, but also trace rain loss [cf. *Sugiura and Yang*, 2003]. (4) A fixed vegetation albedo (as usually applied in NWP and many climate models) and the snow albedo parameterization may contribute to discrepancies.

[30] Reasons for premature freeze-up include: (1) Non-reported snow (depth). *Ling and Zhang* [2003] reported that delaying the snow-cover onset date by ten days can result in a decrease in maximum soil temperature up to 9, 2.9, 2, and 1.1 K and in annual average temperature up to 0.7, 0.5, 0.4, and 0.4 K at the surface, 0.5, 1, and 2 m depth. These values are within the range of our discrepancies. (2) Problems with the downward long-wave radiation measurements and replacing missing values by calculated ones may contribute to premature active layer freezing. Note that *Slater et al.* [1998] reported premature freezing of up to 2 months for the Best Approximation for Surface Exchange scheme [*Desborough*, 1997], related to the parameterization of downward long-wave radiation; *Mölders et al.* [2003a] reported that the frequency of predicted days with frozen ground is very sensitive to the parameterization of downward long-wave radiation. *Schlosser et al.* [2000] and *Mölders et al.* [2003a] also found that the water budget was sensitive to the parameterization of downward long-wave radiation.

[31] Generally, annual averages of RMSEs and SDEs are higher in 1998/99 than for 1993 to 1996, and 2002/03, respectively, which may be due to problems with the new radiation equipment deployed in 1998. In 1998/99 much more missing data had to be replaced by calculations than for other time periods.

[32] Soil moisture measurements are available at 0.10, 0.22, and 0.35 m depth for 2002/03. During this time the groundwater table is around 0.1 m in early summer indicating saturated soil at all soil moisture sensors. Above 0.1 m, predicted volumetric water content of the thawed active layer decreases in summer and refills in fall. As expected for permafrost soils [*Hinkel et al.*, 2001], predicted total relative soil moisture content equals or is close to 1 all year round.

3.3. Soil Thermal Conductivity

[33] Predicted soil temperature is highly sensitive to the thermal conductivity of the ground and snow [e.g., *Zhang et al.*, 1996; *Riseborough*, 2002]. The parameterization of thermal conductivity according to equation (4) provides much higher thermal conductivity values (Figure 3) than typically observed in permafrost soils (e.g., Table 4). Moreover, equation (4) provides a decrease of thermal conductivity as the ground freezes, while typically the opposite is observed (e.g., Table 4). Therefore, we replaced equation (4), which is frequently used in the LSMs of atmospheric models, by *Farouki*'s [1981] parameterization, $\lambda = \lambda_s^{(1-\eta_s)} \lambda_w^{(\eta_s - \eta_{ice})} \lambda_{ice}^{\eta_{ice}}$, which is often applied in permafrost modeling [e.g., *Lachenbruch et al.*, 1982; *Riseborough*, 2002]. Here λ_s (see Table 1 for values), λ_w(=0.57 W/(mK)), and λ_{ice}(=2.31 W/(mK)) are thermal conductivity of dry soil, water, and ice, respectively. We modified this parameterization for model-consistent application in HTSVS as:

$$\lambda = \lambda_s^{(1-\eta_s)} \lambda_w^{\eta} \lambda_{ice}^{\eta_{ice}} \lambda_a^{(\eta_s - \eta - \eta_{ice})} \quad (13)$$

where λ_a(=0.025 W/(mK)) is the thermal conductivity of air. *Farouki*'s formulation neglects the impact of air because permafrost soil pores are typically totally ice-filled. We consider the effect of partly air-filled pores for two reasons: First, consistency with equations (1) to (3) requires inclusion of air, because these equations explicitly consider water vapor fluxes (third and first on the right side of equations (1) and (2), respectively) and air (last term of equation (3)). Second, a LSM for use in NWP and climate models must also describe non-permafrost, partly air-filled soils appro-

Figure 2. Simulated and observed soil temperatures for (a) 1993–1996, (b) 1998/99, and (c) 2002/03 and simulated and observed vertical soil temperature profiles at various seasons for (d) 1993/94, (e) 1994/95, (f) 1995/96, (g) 1998/99, and (h) 2002/03 as obtained by the reference simulation (CTR). CTR uses equation (13) to calculate thermal conductivity. The x-axis in (a), (b), and (c) differ, (a) shows about three years worth of data, (b) and (c) show one freeze-thaw cycle. The y-axis in (d) to (h) differ, because soil temperature measurements were available at eight levels to 1 m depth in the 1990's and at 12 levels up to 1.10 m depth in 2002/03.

Table 4. Soil Thermal Conductivity Determined for Barrow for Thawed and Frozen Soil[a]

	Soil Thermal Conductivity	
Depth, m	Thawed Ground, W/(mK)	Frozen Ground, W/(mK)
0–0.2	0.7	1.4
0.2–1	1.0	1.8
1–2	0.95	1.6
2–12	1.6	2.4
12–34	1.2	1.9

[a]Updated data from *Romanovsky and Osterkamp* [2000].

priately (e.g., in midlatitudes or deserts). Permafrost soils are usually saturated, i.e., $\eta_{air} = \eta_s - \eta - \eta_{ice} = 0$, meaning $\eta_s - \eta_{ice} = \eta$, and $\lambda_a^{(\eta_s-\eta-\eta_{ice})} = \lambda_a^0 = 1$, and equation (13) and Farouki's equation provide identical results.

[34] The HTSVS original formulation generally provides greater thermal conductivity values than the new parameterizations (Figure 3). For our episode thermal conductivity calculated with equation (4) ranges between 0.292 and 5.745 W/(mK); on average, values are about 2.2 W/(mK) and 1.5 W/(mK) in the deeper and upper soil respectively, much higher than values typically measured at Barrow (Table 4). The simulation carried out with equation (13) provided thermal conductivity values between 0.149 (uppermost layer after dry episode) and 1.52 W/(mK); on average, values are about 1.1 W/(mK) between 0.25 and 1.8 m and less than 1 W/(mK) elsewhere, and lower in summer than winter. These values agree well with the range previously determined for frozen and thawed Barrow soil (Table 4). Note that in an uncertainty analysis using Gaussian error propagating techniques, *Mölders et al.* [2005] identified equation (4) as critical because the natural variance in empirical parameters (pore-size distribution index, saturated water potential, porosity) propagates to great uncertainty in calculated thermal conductivity. Uncertainty in equation (13) parameters propagates less strongly leading to less parameter-caused statistical uncertainty in calculated thermal conductivity, soil temperatures, and soil-heat fluxes.

[35] Averaged over all depths, RMSEs are about 3.0 K, 4.8 K and 3.1 K for 1993/96, 1998/99 and 2002/03, in the simulation performed with equation (4). This simulation is denoted CTR-EQ4 hereafter. In the simulation using equation (13), called CTR further on, RMSEs decreased by up to 0.4, 0.2, and 0.2 K on average for 1993–1996, 1998/99, and 2002/03, respectively; by up to 1 K in some layers; and overall by on average 0.2 K (Table 3). Active layer depth is overestimated (up to 0.5 m) in CTR-EQ4, and underestimated (up to 0.3 m) in CTR (see Figures 2 and 4).

[36] In CTR-EQ4, the variance of simulated and observed soil temperature time series differs significantly (at the 95% or higher confidence level) overall (Table 3) and below 0.3 m for all except the last episode. Statistically significant differences only occur for a short time between 0.3 and 0.7 m in CTR. The discrepancies for the latter can be explained by the difficulty in capturing the actual active layer depth on a non-regular grid.

[37] Based on these findings equation (13) should be favored for calculation of thermal conductivity. Therefore, in the following simulations, we use equation (13) and refer

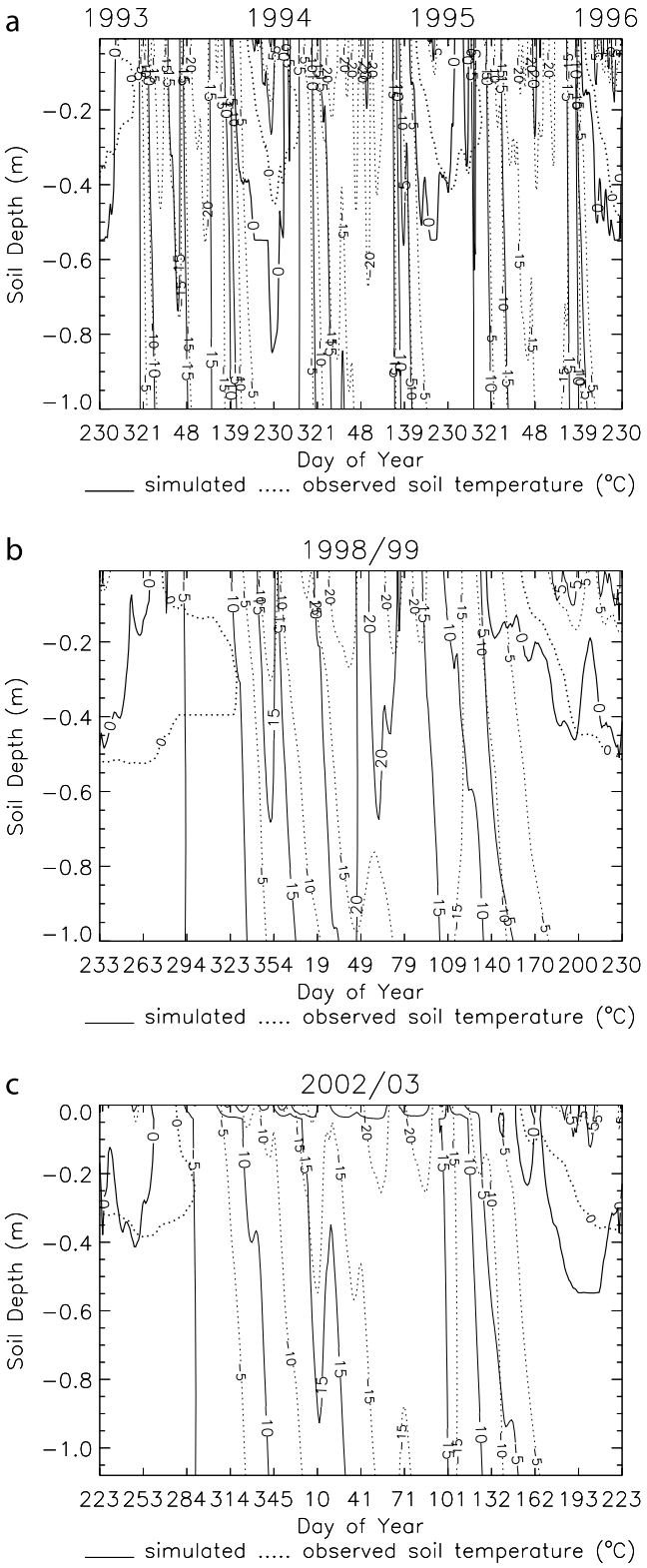

Figure 4. Simulated and observed soil temperatures as obtained by CTR-EQ4 for (a) 1993–1996, (b) 1998/99, and (c) 2002/03. CTR-EQ4 uses equation (4) instead of equation (13) to calculate thermal conductivity.

to the simulation with equation (13) as the reference simulation (CTR).

3.4. Reference Simulation (CTR)

[38] In the reference simulation, soil temperatures and their annual variance are captured better between 0.2 m and 0.3 m and below 0.7 m beneath the surface than elsewhere. Annual RMSEs are highest in the uppermost 0.1 m because variability is greater close beneath the surface than deeper in the soil and hence is more difficult to predict [cf. *Mölders et al.*, 2003b]. Moreover, the possibility that the temperature field is influenced by sensor installation is higher close beneath the surface than deeper in the soil. Discrepancies in variance at depths between 0.3 and 0.7 m are due to incorrect prediction of the active layer depth (Figure 2). Around 1 m depth, soil hydraulic properties change (Table 1), which may contribute to the large RMSEs found here. Uncertainty in the empirical soil physical parameters for gravel causes discrepancies that propagate to the 1 m depth level leading to RMSEs up to 6.8 K at 1.08 m depth in 2002/03. Averaged over all depths, RMSEs are about 2.6, 4.6, and 2.9 K for 1993/96, 1998/99 and 2002/03, respectively.

[39] The model tends to underestimate soil temperatures slightly in winter of 1993/94, 1995/96, and 1998/99, and in late winter of 1994/95 (Figure 2). Early winter soil temperatures are too high in 1994/95. Factors contributing to this deficiency are non-matching thermal conductivity of the snow, and errors in measured long-wave downward radiation.

[40] Predicted soil temperatures are too low in all five summers and falls. The depth of the active layer is usually underestimated (up to 0.3 m) in midsummer. However, the predicted temperature state of the active layer gradually improves close beneath the surface in midsummer (Figure 2). On average, the location of the freezing line is broadly captured during summer within the range of what the grid resolution permits.

[41] The model does not capture the zero-curtain situation (i.e., a layer of unfrozen ground between two layers of frozen ground) between 0.1 and 0.25 m that is observed in fall. Note that this zero curtain situation lasts for an extremely long time in fall 1998 (Figure 2). The reasons given in section 3.2, the vertically coarse resolution (only 12 layers below 1 m depth) and active layer depth underestimation contribute to this failure.

[42] Below the active layer, the seasonal cycle of soil temperature is acceptably captured for all five years of data (Figure 2). In 1998/99, predicted soil temperatures are too low throughout the year except for spring.

3.5. Vertical Resolution

[43] In theory, fine soil grid resolution guarantees accurate simulation of soil temperature and moisture profiles. However, global data sets describing vertical distributions of soil parameters and initial soil temperature and moisture conditions must be available at the same resolution. Thus, availability of these data sets and the huge computational burden associated with a fine grid limit the vertical grid resolution that can be reasonably chosen in NWP or climate models. Consequently, the balance between efficiency and practical accuracy dictates the resolution of soil grids in the LSMs of these models and limits accuracy of soil-temperature predictions. Currently, most of these models use five to ten soil layers [e.g., *Bonan et al.*, 2002; *Stendel and Christensen*, 2002] that cover a depth down to 2 to 3 m [e.g., *Chen and Dudhia*, 2001; *Mölders and Walsh*, 2004].

[44] We examine the impact of the vertical grid resolution to (1) assess the current representation of soil processes in NWP and climate modeling, and (2) recommend an optimum for currently available computational possibilities. To accomplish this we perform simulations using ten layers to cover the first 2, 3, and 20 m beneath the surface, referred to as S10-2, S10-3, and S10-20, respectively. Like CTR these runs are performed with a constant soil temperature of -9.5°C at 20 m depth to minimize the impact of the soil model's lower boundary. For S10-2 and S10-3, this procedure permits non-constant fluxes, soil temperatures and moisture at 2 and 3 m depth, respectively.

3.5.1. Soil Grid

[45] To produce ten layers in the upper 3 m, the model is run with 13 layers (reaching to about 0.01, 0.02, 0.04, 0.07, 0.13, 0.24, 0.45, 0.84, 1.59, 2.99, 5.63, 10.62, and 20 m). Due to the coarser resolution soil temperature profiles predicted by S10-3 show fewer details, and on average RMSEs 0.3, 0.4, and 0.2 K higher for 1993–1996, 1998/98 and 2002/03 than those obtained by CTR (Figures 2 and 5). Compared to CTR, S10-3 captures freezing and thawing and the related release and consumption of heat less well. The variance of the predicted and observed soil temperature time series differs significantly (Table 3), mainly between 0.3 and 0.7 m depth in 1993–1996.

[46] To produce ten layers in the upper 2 m or so, the model is run with 14 layers (reaching to about 0.01, 0.02, 0.03, 0.06, 0.1, 0.19, 0.33, 0.6, 1.07, 1.93, 3.46, 6.21, 11.15, and 20 m). Thus, S10-2 permits more details than S10-3, but less than CTR. Again the coarser resolution reduces prediction accuracy leading to average RMSEs 0.9, 1, and 0.9 K higher than CTR for 1993–1996, 1998/98 and 2002/03. Simulated soil conditions are too warm in late winter and spring 1994, and too cold in late winter 1995, all winter 1995/96 and 1998/1999, fall 2002, and all summers. The variance of simulated and observed soil temperatures differs significantly in the first 0.3 m beneath the surface.

[47] Using ten layers to a depth of 20 m (reaching to about 0.01, 0.02, 0.05, 0.13, 0.29, 0.68, 1.59, 3.69, 8.60, and 20 m) affects the RMSE slightly. Occasionally the variance of simulated and observed soil temperature differs significantly between 0.3 and 0.7 m depth in 1993–1996 and below 0.7 m in 2002/03, but not on average (Table 3).

[48] Evidently, the number and position of the grid nodes play a role in capturing the active layer depth. This fact is also manifested by the change in bias (Table 3). Discrepancies of 0.2 to 1 K between simulations and observations can be caused by grid resolution with impact on the simulated temperature variation. The findings imply that a compromise between the number of grid layers and the depth of the lower soil model boundary on one side and the amount of computational time on the other has to be made, which is easier on a logarithmic grid than on the equally spaced grid typically used in permafrost modeling. Interestingly, the impact of a coarse resolution in the deep soil levels is on average higher in winter than summer.

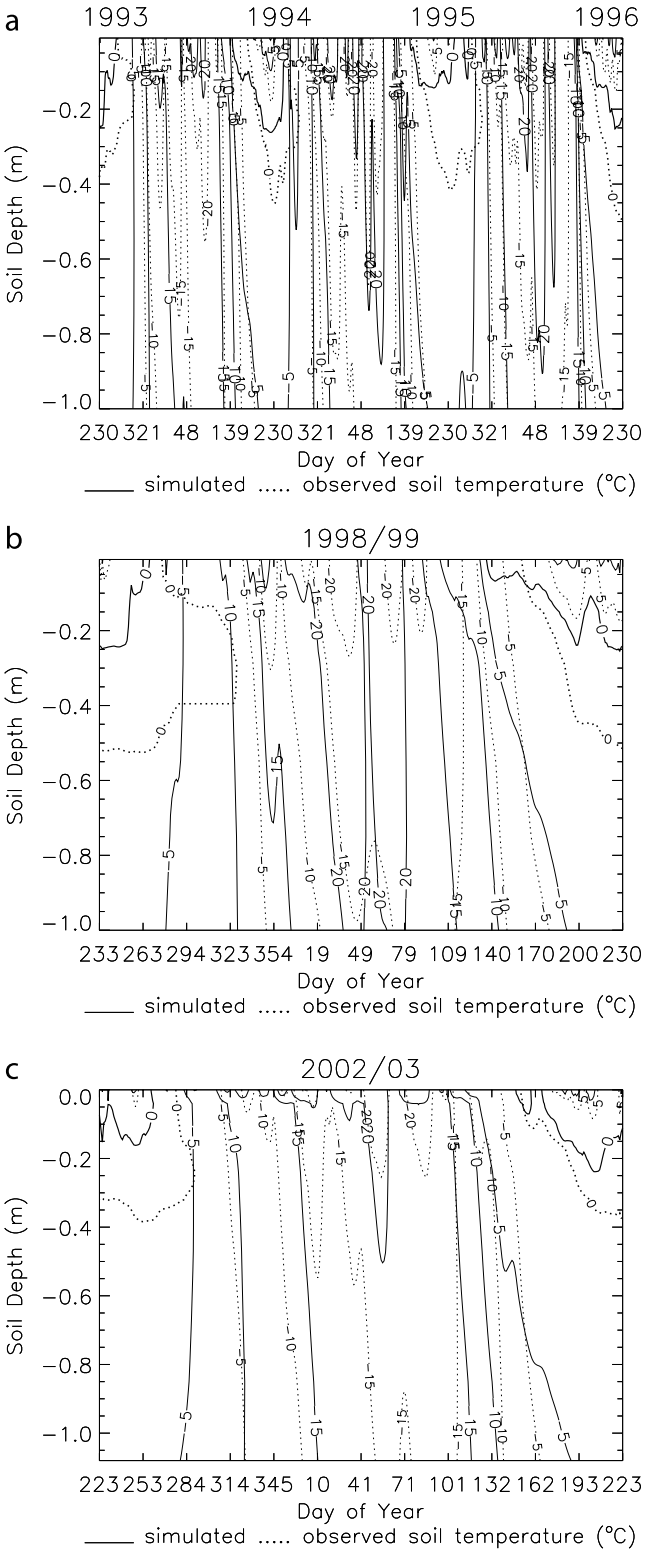

Figure 5. Like Figure 4, but as obtained by S3-10. S3-10 uses 13 layers to a depth of 20 m to obtain 10 layers to 3 m depth.

3.5.2. Soil Characteristics Profile

[49] Most modern soil models used in atmospheric NWP or climate models assume one soil type for the entire soil column [e.g., *Slater et al.*, 1998; *Schlosser et al.*, 2000]. To examine the impact of this assumption, a sensitivity study (SHOM) was performed wherein the parameters of the uppermost soil layer were used for the entire soil column. The simulated soil temperature pattern misses many details that result from the vertical profile of soil parameters (Figures 2 and 6). As compared to CTR, and even in the uppermost layer where the soil type remained the same, RMSEs increased on average by 0.1, 0.4, and 0.3 K for 1993–1996, 1998/99 and 2002/03. The variance of simulated and observed soil temperature time series differs significantly (Table 3). While for 1993–1996 soil temperatures close beneath the surface are too high during winter, they are too low in the winters of 1998/99 and 2002/2003. Summer soil temperatures that are too low lead to an underestimation of the active layer depth (up to 0.4 m).

3.6. Lower Boundary

[50] Ideally, the bottom of a soil model is placed at a level of constant soil temperature and moisture states as in our reference run at 20 m depth. Most modern soil models used in NWP or climate models typically set their lower boundary around 2 or 3 m depth [e.g., *Chen and Dudhia*, 2001; *Mölders and Walsh*, 2004]. In permafrost soils, however, seasonal and decadal variations in soil temperature exist even below 15 m depth [*Romanovsky et al.*, 1997]. Thus, using a constant soil temperature at the bottom of a soil model at 2 or 3m depth is generally impractical in climate modeling, as it introduces artificial sources and sinks for heat and moisture [e.g., *Stendel and Christensen*, 2002]. For the typical forecast range of NWP (several days) a constant lower boundary condition can be suitable if appropriately set [e.g., *Narapusetty and Mölders*, 2005]. Typically, NWP models use a prescribed fixed climatologic temperature, which varies monthly and spatially, as a lower boundary condition. In contrast, climate models usually assume zero-flux conditions at the lower boundary of the soil model [*Oleson et al.*, 2004]. However, zero heat and moisture flux must not necessarily exist at 2 or 3 m depths [e.g., *Zhang et al.*, 1996; *Romanovsky et al.*, 1997; *Mölders et al.*, 2003a, 2003b].

[51] Sensitivity studies, called SB2L10 and SB3L10 hereafter, were carried out with ten layers wherein the lower boundary condition varied according to a climatologic annual course at 2 and 3 m depth. A further simulation, SB3L5, used five layers and climatologic data at 3 m depth. Note that for climate change scenarios climatologic values cannot be used as a lower boundary condition because they may alter with climate.

[52] If there are ten layers in the upper 3 m (reaching to about 0.01, 0.02, 0.04, 0.07, 0.13, 0.24, 0.45, 0.84, 1.59 and 3 m), the grid will be coarser than that of CTR in the first 3 m beneath the surface. As evidenced by the RMSEs, bias, and SDEs (Table 3), changing the position of grid nodes also affects how accurately different soil layer characteristics can be resolved. In SB3L10, RMSEs decrease on average by 0.1, 0.7, and 0.5 K for 1993–1996, 1998/99, and 2002/03 as compared to CTR. Obviously, the climatologic values at 3 m depth capture conditions in 1998/99 and 2002/03 better than those in 1993–1996 and hence explain the greater improvement for these episodes than for the 1993/96 episode. In early summer of 2003, the active layer depth and its temporal evolution is excellently predicted, and in

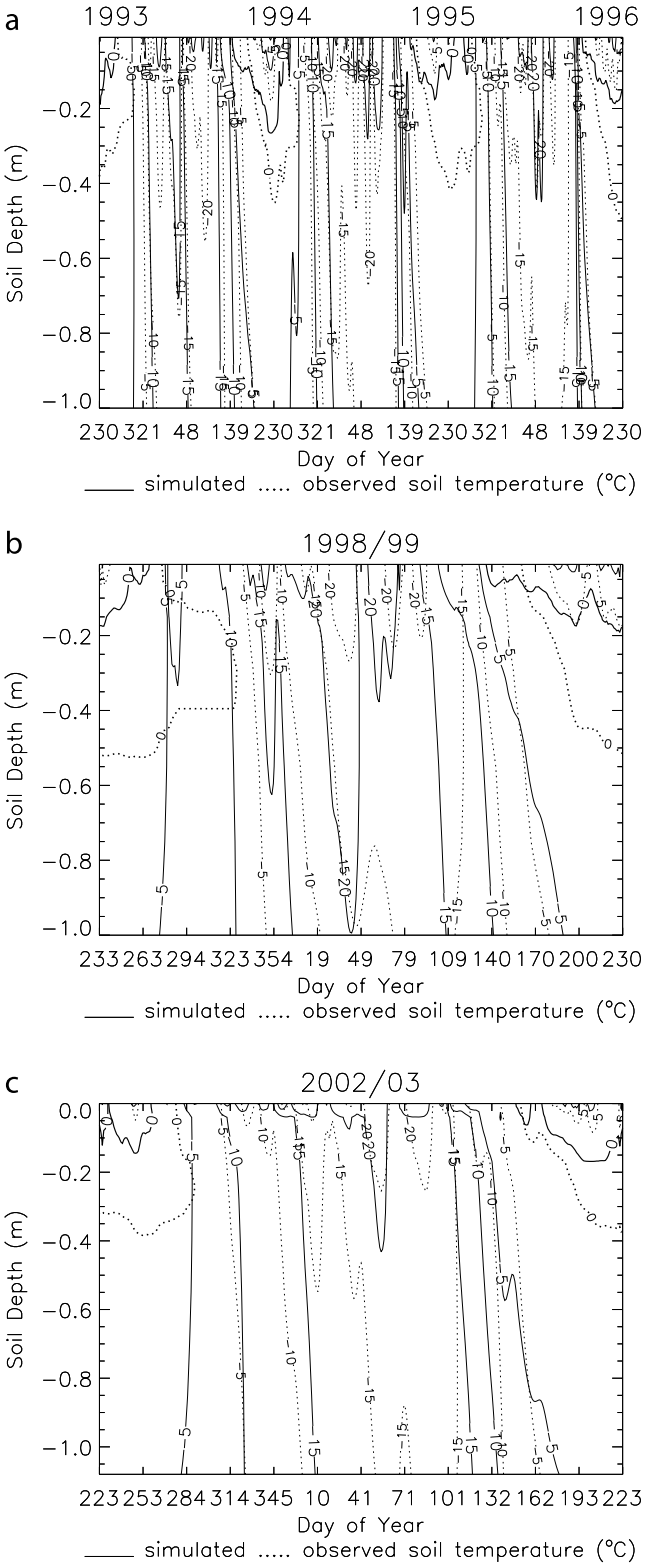

Figure 6. Like Figure 4, but as obtained by SHOM. SHOM assumes silt with organics for the entire soil column.

summer of 1994 and 1999, the maximum active layer depth is excellently captured (Figure 7). The bias, which includes contributions of systematic errors due to the grid position, decreases by an order of magnitude (Table 3). These facts indicate that the improvement is due to the position of the soil model layers relative to the actual active layer depth in this simulation rather than to the treatment of the boundary conditions. Obviously, if a soil-model grid layer is close to the active layer depth, the chance to capture the active layer depth correctly increases. In three-dimensional NWP and climate-model applications, however, the soil grid cannot be chosen in order to optimally capture maximum active layer depth, especially as active layer depth varies strongly in space and slightly in time.

[53] Despite the overall improvement (Table 3), the variance of simulated and observed soil temperature time series differs significantly between 0.3 and 0.7 m, but not on average. As compared to the observations, neglecting deeper soil conditions leads to soil conditions that are slightly too warm overall (positive bias), except for 1998/99 and all summers (Figure 7).

[54] If there are ten layers to 2 m depth (reaching to about 0.01, 0.02, 0.03, 0.06, 0.11, 0.19, 0.34, 0.62, 1.1 and 2 m), the grid will be coarser than in CTR, but finer than in SB3L10. On average, RMSEs will increase by 0.1 K for 1993–1996 and 1998/98, and decrease by 0.1 K for 2002/03 as compared to CTR. The variance of simulated and observed soil temperature time series differs significantly (Table 3), especially in the first 0.1 m beneath the surface. Predicted summer soil conditions are cooler than observed. In summers of 1994, 2002, and 2003, the maximum active layer depth is accurately captured for the same reasons as for SB3L10. In winter, SB2L10 predicts warmer than observed soil conditions except for 1998/99. The slightly increased SDE (Table 3) indicates that the prescribed climatologic data cause errors at the lower boundary.

[55] If only five layers exist to 3 m depth (reaching to about 0.01, 0.04, 0.17, 0.72, and 3 m), the active layer is as much as 0.35 m too deep. Variances of simulated and observed soil temperature time series differ significantly (Table 3), especially in the first 0.3 m beneath the surface. As compared to CTR, SB3L5 produces RMSEs that are, on average, 0.2 and 0.1 K too high for 1993/96 and 1998/99 respectively, and 0.2 K too low for 2002/03.

[56] These findings suggest that prescribed monthly climatologic values may be an option for NWP models, but carry the danger of a heat source or sink artifact if the actual temperatures are lower or higher at that depth. They also imply that the number and position of grid nodes play a role in accurately capturing the active layer depth.

3.7. Snow Treatment

[57] Various authors have demonstrated the thermo-insulation effect of snow on soil temperatures and energy balance [e.g., *Zhang et al.*, 1996, 1997; *Fröhlich and Mölders*, 2002; *Sokratov and Barry*, 2002; *Mölders and Walsh*, 2004]. Thermal conductivity of the snowpack depends on snow characteristics and is usually parameterized as density dependent [e.g., *Sturm et al.*, 1997; *Mölders and Walsh*, 2004]. Since no observations of snow thermal conductivity, snow density or snowfall were available, it was necessary to make assumptions about snowpack properties as described in section 2.4. To assess the impact on results, we performed several sensitivity studies.

[58] Our snow thermal conductivity value (0.14 W/(mK)) is typical for fresh rather than old snow [e.g., *Lee*, 1978;

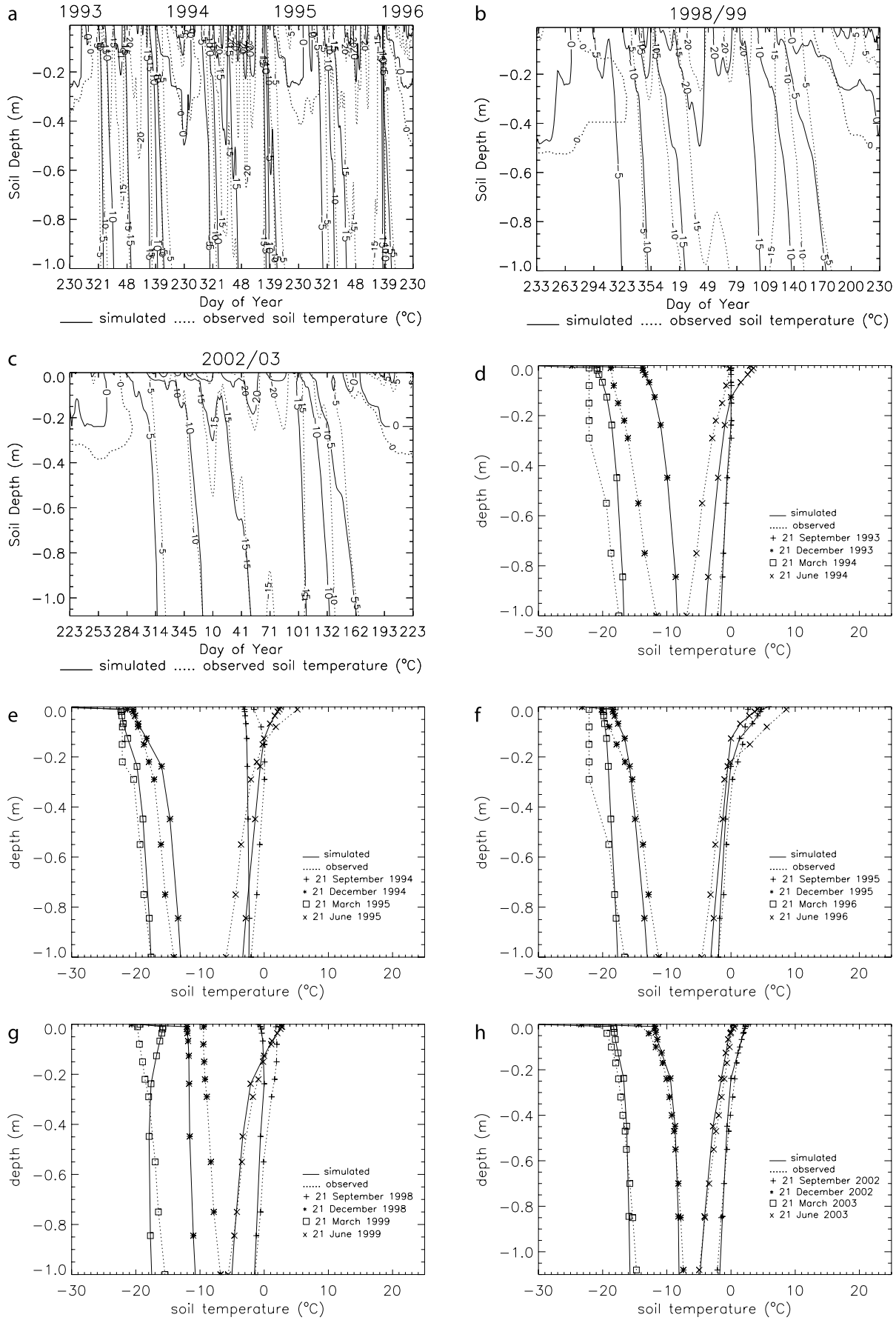
a
1993
1994
1995
1996
Soil Depth (m)
Day of Year
simulated ..... observed soil temperature (°C)
b
1998/99
Soil Depth (m)
Day of Year
simulated ..... observed soil temperature (°C)
c
2002/03
Soil Depth (m)
Day of Year
simulated ..... observed soil temperature (°C)
d
depth (m)
soil temperature (°C)
simulated
observed
+ 21 September 1993
* 21 December 1993
□ 21 March 1994
x 21 June 1994
e
depth (m)
soil temperature (°C)
simulated
observed
+ 21 September 1994
* 21 December 1994
□ 21 March 1995
x 21 June 1995
f
depth (m)
soil temperature (°C)
simulated
observed
+ 21 September 1995
* 21 December 1995
□ 21 March 1996
x 21 June 1996
g
depth (m)
soil temperature (°C)
simulated
observed
+ 21 September 1998
* 21 December 1998
□ 21 March 1999
x 21 June 1999
h
depth (m)
soil temperature (°C)
simulated
observed
+ 21 September 2002
* 21 December 2002
□ 21 March 2003
x 21 June 2003

Figure 7

Sturm et al., 1997]. Assuming a value of 0.42 W/(mK) that is typical for old snow [*Oke*, 1987] increases RMSE on average by 1, 0.9, and 0.5 K for 1993–1996, 1998/99 and 2002/03. As compared to observations, soil temperatures predicted by this simulation (called SNWTHC) are generally too cold except for the upper soil in spring. Time series of predicted and observed soil temperature variance differ significantly (Table 3). The increased bias indicates that the systematic error grows with this assumption. Generally increasing thermal conductivity leads to colder soil conditions and vice versa with some impact on onset of active layer thawing and depth in summer. These results agree well with those found by *Zhang et al.* [1996] using a permafrost model. We conclude that some thermal accuracy arises from using a fixed value for thermal conductivity.

[59] A 10% increase of snow depth (simulation SNWHS) changes RMSEs by ±0.1 K, on average. A similar result is found for decreasing snow depth by 10%. Thus, snow depth discrepancies of less than ±10% between soil temperature and snow depth sites will only slightly affect RMSE. However, stopping snow depth reports too early or starting them too late will have a much higher impact on soil temperature [cf. *Ling and Zhang*, 2003], and snow depth can vary strongly in space due to snow blowing [*Yang and Woo*, 1999].

[60] A sensitivity study (S5SNL) wherein the number of snow layers was increased from three to five layers showed no improvement in soil temperature prediction. The increased RMSE (0.1, 0.3, 0.1 K for 1993–1996, 1998/99, 2002/03) suggests that for thin snowpacks like those in Barrow a low vertical resolution of the snow model grid will be sufficient if the vertical structure of snow thermal conductivity is neglected.

3.8. Albedo

[61] HTSVS uses a constant value for vegetation albedo from right after snowmelt until snowfall. In nature, however, vegetation albedo strongly varies during the growth season. Since net radiation is partitioned between sensible and latent heat fluxes and ground heat flux, the choice of vegetation albedo will influence soil temperature and moisture states. *Mölders et al.* [2003b] reported that for a 10% increase in albedo the 2050 days total of evapotranspiration and recharge can differ up to 211 mm and 43 mm, respectively.

[62] Sensitivity studies suggest that warming and thawing and the temperature of the active layer is overestimated in the first weeks after snowmelt because the albedo of dead tundra grass is higher than for freshly grown tundra grass.

[63] Using *Mölders et al.*'s [2003a] parameterization of snow albedo for $T < 0°C$ (SALB) leads to on average a 0.1 K higher RMSE for 1993–1996 and 2002/03, and 0.1 K lower RMSE for 1998/99 than CTR. Note that for $T < 0°C$ *Mölders et al.'s* [2003a] parameterization usually provides higher albedo values immediately after, and lower values long after a snow event than does *Luijting et al.*'s [2004] parameterization. On average, using the former parameterization yields soil temperatures that are too cold year round and underestimates the active layer depth by up to 0.35 m, but captures the zero curtain condition in fall 1993. We conclude that some of the discrepancies in soil temperature prediction found may result from the treatment of albedo.

4. Conclusions

[64] We examined HTSVS' ability to simulate long-term permafrost and active layer thermodynamics using observations collected at Barrow, Alaska, a cold permafrost site. HTSVS runs without calibration and without restart, driven with meteorological observations available from 1 January 1990 to 31 December 2003. HTSVS was started with climatologic soil temperature values assuming a saturated soil. The model was forced by 1990 data, repeating that year three times to reach equilibrium between soil temperatures, volumetric water and ice content and climate (model spin-up). Differences between soil temperature predicted for the first and second year are less than 0.5 K after only 1 day. Results from a simulation with and without this spin-up procedure hardly differ. This means the frozen ground/permafrost model "forgets" the initial state rapidly, responds well to atmospheric forcing, and can be considered for use in climate variability and change studies.

[65] Simulated soil temperatures were compared to observations available for 1993–96, 1998/1999, and 2002/2003. HTSVS predicts soil temperatures within 3.2 K accuracy, on average. Soil temperature predictions are the best for relatively warm years with relatively thick snowpacks. They are the worst for years of low annual mean snow depth and air temperature, because errors in snow thermal conductivity, snow depth and radiation measurements have greater influence on predicted soil temperature. This means that modeling permafrost in climate models requires good snow models.

[66] Sensitivity studies showed that errors in reported snow depth and duration, rain and radiation measurements, assumptions about diurnal precipitation distribution, and various parameters (e.g., albedo, snow thermal conductivity) cause errors in predicted soil temperatures. Snow thermal conductivity exerts an indirect impact after snow-melt. The choices of soil thermal conductivity parameterization, lower boundary condition, and vertical grid resolution have the greatest impact on simulated soil temperature accuracy. The accuracy of predicted active layer depth strongly depends on model resolution and the proximity of the freezing line to the position of a grid node. The soil-grid design can lead to both over- and under-prediction of soil temperatures and active layer depth. Here especially the number of layers plays a role. Accuracy of predicted active layer depth also depends on the depth of the soil model's lower boundary. Thus, we conclude that a higher resolution in the upper soil beneath the surface (>15 layers) and a deeper location of the soil model boundary than currently applied in most NWP and climate models is desirable.

[67] The results imply that the use of adequately chosen monthly and spatially varying climatologic values at 2 or

Figure 7. Like Figure 2, but for SB3L10. SB3L10 uses ten soil layers and climatologic soil temperature values at 3 m depth.

3 m depth provide acceptable results for NWP. However, this is not an option for climate models as these values change with climate.

[68] In soils with a high fraction of organic material or organic soils, model hydrological predictive skill may arise from the action of a snowpack as an integrator of hydrological processes. If the model is driven with observed snow depth, deficiencies in measured snow depth may lead to a predicted snow density that is too low, resulting in water infiltration that is too low. Since in the model melt-water is assumed to be at 0°C, it will heat the frozen ground as it infiltrates and percolates through pores that are not totally ice-filled, and will also increase soil volumetric heat capacity. Model hydrological predictive skill requires future examination.

[69] At Barrow, the groundwater table is about 0.1 m deep. For sites with deeper groundwater tables rain catch deficiencies, trace precipitation, snow-rain or snow that immediately melts after reaching the ground (and therefore is reported neither as rain nor as snow depth) may contribute to discrepancies between observed and simulated active layer depth, because these trace losses affect soil hydrological conditions and soil temperature. Furthermore, percolating water transports heat, and raises soil volumetric heat capacity. This effect requires further investigation at sites with deeper groundwater tables than at Barrow.

[70] Future studies should also examine the decadal behavior of permafrost in response to climate variability, and the HTSVS performance for warm permafrost as well as the feasibility of the HTSVS frozen ground/permafrost module in a climate model framework.

[71] **Acknowledgments.** We thank S.-I. Akasofu, U. S. Bhatt, G. Kramm, B. Narapusetty, C. O'Connor, M. Shulski, J. E. Walsh, G. Wendler, and the anonymous reviewers for helpful discussion and comments, and NSF for financial support under contract OPP-0327664.

References

Beringer, J., A. H. Lynch, F. S. Chapin III, and M. Mack (2001), The representation of Arctic soils in the land surface model: The importance of mosses, *J. Clim.*, *14*, 3324–3335.

Bonan, G. B., K. W. Oleson, M. Vertenstein, S. Levis, X. Zeng, Y. Dai, R. E. Dickinson, and Z.-L. Yang (2002), The Land Surface Climatology of the Community Land Model coupled to the NCAR Community Climate Model, *J. Clim.*, *15*, 1115–1130.

Chen, F., and J. Dudhia (2001), Coupling an advanced land surface hydrology model with the Penn State/NCAR MM5 modeling system. Part I: Model implementation and sensitivity, *Mon. Weather Rev.*, *129*, 569–585.

Cherkauer, K. A., and D. P. Lettenmaier (1999), Hydrologic effects of frozen soils in the upper Mississippi river basin, *J. Geophys. Res.*, *104*, 19,611–19,621.

Clapp, R. B., and G. M. Hornberger (1978), Empirical equations for some soil hydraulic properties, *Water Resour. Res.*, *14*, 601–604.

Deardorff, J. W. (1978), Efficient prediction of ground surface temperature and moisture, with inclusion of a layer of vegetation, *J. Geophys. Res.*, *83*, 1889–1903.

de Groot, S. R. (1951), *Thermodynamics of Irreversible Processes*, 242 pp., Wiley-Interscience, Hoboken, N. J.

Desborough, C. E. (1997), The impact of root-weighting on the response of transpiration to moisture stress in a land surface scheme, *Mon. Weather Rev.*, *125*, 1920–1930.

de Vries, D. A. (1958), Simultaneous transfer of heat and moisture in porous media, *Eos Trans. AGU*, *39*, 909–916.

Dingman, S. L. (1994), *Physical Hydrology*, 575 pp., Macmillan, New York.

Ellingson, R. G., K. Stamnes, J. A. Curry, J. E. Walsh, and B. D. Zak (1999), Overview of North Slope of Alaska/adjacent Arctic Ocean science issues, *J. Clim.*, *12*, 46–63.

Entekhabi, D., and K. L. Brubaker (1995), An analytical approach to modeling land-atmosphere interaction: 2. Stochastic formulation, *Water Resour. Res.*, *31*, 633–643.

Eppel, D. P., H. Kapitza, M. Claussen, D. Jacob, W. Koch, L. Levkov, H.-T. Mengelkamp, and N. Werrmann (1995), The non-hydrostatic mesoscale model GESIMA. Part II: Parameterizations and applications, *Contrib. Atmos. Phys.*, *68*, 15–41.

Esch, D. C., and T. E. Osterkamp (1990), Cold region engineering: Climatic warming concerns for Alaska, *J. Cold Reg. Eng.*, *4*(1), 6–14.

Farouki, O. (1981), Thermal properties of soils, *CRREL Monogr. 81-1*, U.S. Army Cold Reg. Res. and Eng. Lab., Hanover, N. H.

Flerchinger, G. N., and K. E. Saxton (1989), Simultaneous heat and water model of a freezing snow-residue-soil system I. Theory and development, *Trans. ASAE*, *32*, 565–571.

Fröhlich, K., and N. Mölders (2002), Investigations on the impact of explicitly predicted snow metamorphism on the microclimate simulated by a meso-β/γ-scale non-hydrostatic model, *Atmos. Res.*, *62*, 71–109.

Goodrich, W. E. (1982), The influence of snow cover on the ground thermal regime, *Can. Geotech. J.*, *19*, 421–432.

Hinkel, K. M., R. F. Paetzold, F. E. Nelson, and J. G. Bockheim (2001), Patterns of soil temperature and moisture in the active layer and upper permafrost at Barrow, Alaska: 1993–1999, *Global Planet. Change*, *29*, 293–309.

Hinkel, K. M., F. E. Nelson, A. E. Klene, and J. H. Bell (2003), The urban heat island in winter at Barrow, Alaska, *Int. J. Climatol.*, *23*(15), 1889–1905.

Kane, D. L., L. D. Hinzman, and J. P. Zarling (1991), Thermal response of the active layer in a permafrost environment to climatic warming, *Cold Reg. Sci. Technol.*, *19*(2), 111–122.

Kramm, G. (1995), *Zum Austausch von Ozon und reaktiven Stickstoffverbindungen zwischen Atmosphäre und Biosphäre*, p. 268, Maraun-Verlag, Frankfurt, Germany.

Kramm, G., R. Dlugi, N. Mölders, and H. Müller (1994), Numerical investigations of the dry deposition of reactive trace gases, in *Computer Simulation, Air Pollution II*, vol. 1, edited by J. M. Baldasano et al., pp. 285–307, Comput. Mech., Billerica, Mass.

Kramm, G., N. Beier, T. Foken, H. Müller, P. Schröder, and W. Seiler (1996), A SVAT scheme for NO, NO_2, and O_3 - Model description, *Meteorol. Atmos. Phys.*, *61*, 89–106.

Lachenbruch, A. H., J. H. Sass, B. V. Marshall, and T. H. Moses (1982), Permafrost, heat flow, and the geothermal regime at Prudhoe Bay, Alaska, *J. Geophys. Res.*, *87*(B11), 9301–9316.

Lee, R. (1978), *Forest Micrometeorology*, Columbia Univ. Press, New York.

LeMone, M. A., et al. (2000), Land-atmosphere interaction research, early results and opportunities in the Walnut river watershed in southeast Kansas: CASES and ABLE, *Bull. Am. Meteorol. Soc.*, *81*, 757–779.

Ling, F., and T. Zhang (2003), Impact of the timing and duration of seasonal snow cover on the active layer and permafrost in the Alaskan Arctic, *Permafrost Periglac. Process.*, *14*, 141–150.

Luijting, H., N. Mölders, and K. Sassen (2004), Temporal behavior of snow albedo at the Barrow ARM site in Alaska, M.S. research internship report, 36 pp., Univ. of Alaska Fairbanks, Fairbanks, Alaska.

Luo, L., et al. (2003), Effects of frozen soil on soil temperature, spring infiltration, and runoff: Results from the PILPS2 (d) experiment at Valdai, Russia, *J. Hydrometeorol.*, *4*, 334–351.

McCumber, M. C. (1980), A numerical simulation of the influences of heat and moisture fluxes upon mesoscale circulation, Ph.D. thesis, Dep. of Environ. Sci., Univ. of Va., Charlottesville.

Mölders, N. (2000), HTSVS - A new land-surface scheme for MM5, paper presented at Tenth PSU/NCAR Mesoscale Model Users' Workshop, Natl. Cent. for Atmos. Res., Boulder, Colo.

Mölders, N., and A. Raabe (1997), Testing the effect of a two-way-coupling of a meteorological and a hydrologic model on the predicted local weather, *Atmos. Res.*, *45*, 81–108.

Mölders, N., and J. E. Walsh (2004), Atmospheric response to soil-frost and snow in Alaska in March, *Theor. Appl. Climatol.*, *77*, 77–105.

Mölders, N., A. Raabe, and T. Beckmann (1999), A technique to downscale meteorological quantities for use in hydrologic models - Description and first results, *IAHS Publ.*, *254*, 89–98.

Mölders, N., U. Haferkorn, J. Döring, and G. Kramm (2003a), Long-term numerical investigations on the water budget quantities predicted by the hydro-thermodynamic soil vegetation scheme (HTSVS) – Part I: Description of the model and impact of long-wave radiation, roots, snow, and soil frost, *Meteorol. Atmos. Phys.*, *84*, 115–135.

Mölders, N., U. Haferkorn, J. Döring, and G. Kramm (2003b), Long-term numerical investigations on the water budget quantities predicted by the hydro-thermodynamic soil vegetation scheme (HTSVS) – Part II: Evaluation, sensitivity, and uncertainty, *Meteorol. Atmos. Phys.*, *84*, 137–156.

Mölders, N., M. Jankov, and G. Kramm (2005), Application of Gaussian error propagation principles for theoretical assessment of model uncertainty in simulated soil processes caused by thermal and hydraulic parameters, *J. Hydrometeorol.*, *6*, 1045–1062.

Narapusetty, B., and N. Mölders (2005), Evaluation of snow depth and soil temperature predicted by the Hydro-Thermodynamic Soil-Vegetation Scheme (HTSVS) coupled with the PennState/NCAR Mesoscale Meteorological Model (MM5), *J. Appl. Meteorol.*, *44*, 1827–1843.

Nelson, F., and S. I. Outcalt (1987), Anthropogenic geomorphology in northern Alaska, *Phys. Geogr.*, *3*(1), 17–48.

Oechel, W. C., G. L. Vourlitis, S. J. Hastings, R. C. Zulueta, L. Hinzman, and D. Kane (2000), Acclimation of ecosystem CO_2 exchange in the Alaskan Arctic in response to decadal climate warming, *Nature*, *406*, 978–981.

Oke, T. R. (1987), *Boundary Layer Climates*, 435 pp., Methuen, New York.

Oleson, K. W., et al. (2004), Technical description of the Community Land Model (CLM), *NCAR Tech. Note NCARTN-461+STR*, 174 pp., Natl. Cent. for Atmos. Res., Boulder, Colo.

Osterkamp, T. E., and V. E. Romanovsky (1997), Freezing of the active layer on the Coastal Plain of the Alaskan Arctic, *Permafrost Periglac. Process.*, *8*(1), 23–44.

Osterkamp, T. E., and V. E. Romanovsky (1999), Evidence for warming and thawing of discontinuous permafrost in Alaska, *Permafrost Periglac. Process.*, *10*(1), 17–37.

Philip, J. R., and D. A. de Vries (1957), Moisture in porous materials under temperature gradients, *Trans. Am. Geophys. Soc.*, *18*, 222–232.

Prigogine, I. (1961), *Introduction to Thermodynamics of Irreversible Processes*, 119 pp., Wiley-Interscience, Hoboken, N. J.

Raschke, E., U. Karstens, R. Nolte-Holube, R. Brandt, H.-J. Isemer, D. Lohmann, M. Lobmeyer, B. Rockel, and R. Stuhlmann (1998), The Baltic Sea Experiment BALTEX: A brief overview and some selected results of the authors, *Geophysics*, *19*, 1–22.

Riseborough, D. W. (2002), The mean annual temperature at the top of permafrost, the TTOP model, and the effect of unfrozen water, *Permafrost Periglac. Process.*, *13*, 137–143.

Romanovsky, V. E., and T. E. Osterkamp (1997), Thawing of the active layer on the coastal plain of the Alaskan Arctic, *Permafrost Periglac. Process.*, *8*, 1–22.

Romanovsky, V. E., and T. E. Osterkamp (2000), Effects of unfrozen water on heat and mass transport processes in the active layer and permafrost, *Permafrost Periglac. Process.*, *11*, 219–239.

Romanovsky, V. E., and T. E. Osterkamp (2001), Permafrost: changes and impacts, in *Permafrost Response on Economic Development, Environmental Security and Natural Resources*, edited by R. Paepe and V. Melnikov, pp. 297–315, Springer, New York.

Romanovsky, V. E., T. E. Osterkamp, and N. Duxbury (1997), An evaluation of three numerical models used in simulations of the active layer and permafrost temperature regimes, *Cold Reg. Sci. Technol.*, *26*, 195–203.

Romanovsky, V. E., M. Burgess, S. Smith, K. Yoshikawa, and J. Brown (2002), Permafrost temperature records: Indicators of climate change, *Eos Trans. AGU*, *83*(50), 589–594.

Sasamori, T. (1970), A numerical study of atmospheric and soil boundary layers, *J. Atmos. Sci.*, *27*, 1122–1137.

Schlosser, C. A., et al. (2000), Simulations of a boreal grassland hydrology at Valdai, Russia: PILPS phase 2(d), *Mon. Weather Rev.*, *128*, 301–321.

Serreze, M. C., J. E. Walsh, F. S. Chapin III, T. E. Osterkamp, M. Dyurgerov, V. E. Romanovsky, W. C. Oechel, J. Morison, T. Zhang, and R. G. Barry (2000), Observational evidence of recent change in the northern high-latitude environment, *Clim. Change*, *46*, 159–207.

Sievers, U., R. Forkel, and W. Zdunkowski (1983), Transport equations for heat and moisture in the soil and their application to boundary-layer problems, *Contrib. Atmos. Phys.*, *56*, 58–83.

Slater, A. G., A. J. Pitman, and C. E. Desborough (1998), Simulation of freeze-thaw cycles in a general circulation land surface scheme, *J. Geophys. Res.*, *103*, 11,303–11,312.

Smith, M. W., and D. W. Riseborough (2001), Climate and the limits of permafrost: A zonal analysis, *Permafrost Periglac. Process.*, *13*(1), 1–15.

Sokratov, S. A., and R. G. Barry (2002), Intraseasonal variation in the thermoinsulation effect of snow cover on soil temperatures and energy balance, *J. Geophys. Res.*, *107*(D10), 4093, doi:10.1029/2001JD000489.

Spindler, G., N. Mölders, J. Hansz, N. Beier, and G. Kramm (1996), Determining the dry deposition of SO_2, O_3, NO, and NO_2 at the SANA core station Melpitz, *Meteorol. Z.*, *5*, 205–220.

Stendel, M., and J. H. Christensen (2002), Impact of global warming on permafrost conditions in a coupled GCM, *Geophys. Res. Lett.*, *29*(13), 1632, doi:10.1029/2001GL014345.

Sturm, M., J. Holmgren, M. König, and K. Morris (1997), The thermal conductivity of seasonal snow, *J. Glaciol.*, *43*, 26–41.

Sugiura, K., and D. Yang (2003), Systematic error aspects of gauge-measured solid precipitation in the Arctic, Barrow, Alaska, *Geophys. Res. Lett.*, *30*(4), 1192, doi:10.1029/2002GL015547.

U.S. Army Corps of Engineers (1956), Snow hydrology: Summary report of the snow investigations, *PB 151660*, 462 pp., Off. of Tech. Serv., U.S. Dep. of Commer., Washington, D. C.

Yang, D., and M. K. Woo (1999), Representativeness of local snow data for large-scale hydrological investigations, *Hydrol. Processes*, *13*, 1977–1988.

Yang, D., D. L. Kane, L. D. Hinzman, B. E. Goodison, J. R. Metcalfe, P. Y. T. Louie, G. H. Leavesley, D. G. Emerson, and C. L. Hanson (2000), An evaluation of the Wyoming gauge system for snowfall measurement, *Water Resour. Res.*, *36*(9), 2665–2677.

Yoshikawa, K., V. E. Romanovsky, N. Duxbury, J. Brown, and A. Tsapin (2004), The use of geophysical methods to discriminate between brine layers and freshwater taliks in permafrost regions, *J. Glaciol. Geocryol.*, *26*, 301–309.

Zdunkowski, W. G., J. Paegle, and J. P. Reilly (1975), The effect of soil moisture upon the atmospheric and soil temperature near the air-soil interface, *Arch. Meteorol. Geophys. Bioklimatol.*, *24A*, 245–268.

Zhang, T., T. E. Osterkamp, and K. Stamnes (1996), Influence of the depth hoar layer of the seasonal snow cover on the ground thermal regime, *Water Resour. Res.*, *32*, 2075–2086.

Zhang, T., T. E. Osterkamp, and K. Stamnes (1997), Effect of climate on the active layer and permafrost on the North Slope of Alaska, U.S.A, *Permafrost Periglac. Process.*, *8*, 45–67.

Zhuang, Q., V. E. Romanovsky, and A. D. McGuire (2001), Incorporation of a permafrost model into a large-scale ecosystem model: Evaluation of temporal and spatial scaling issues in simulating soil thermal dynamics, *J. Geophys. Res.*, *106*, 33,649–33,670.

N. Mölders and V. E. Romanovsky, Geophysical Institute, University of Alaska Fairbanks, 903 Koyukuk Drive, P.O. Box 757320, Fairbanks, AK 99775-7320, USA. (molders@gi.alaska.edu)